JOURNAL OF GEOPHYSICAL RESEARCH, VOL. 104, NO. D22, PAGES 27,789–27,801, NOVEMBER 27, 1999

Sensitivity of boreal forest regional water flux and net primary production simulations to sub-grid-scale land cover complexity

J. S. Kimball and S. W. Running

Numerical Terradynamic Simulation Group, School of Forestry, University of Montana, Missoula

S. S. Saatchi

NASA Jet Propulsion Laboratory, Pasadena, California

Abstract. We use a general ecosystem process model (BIOME-BGC) coupled with remote sensing information to evaluate the sensitivity of boreal forest regional evapotranspiration (ET) and net primary production (NPP) to land cover spatial scale. Simulations were conducted over a 3 year period (1994–1996) at spatial scales ranging from 30 to 50 km within the BOREAS southern modeling subarea. Simulated fluxes were spatially complex, ranging from 0.1 to 3.9 Mg C ha^{-1} yr^{-1} and from 18 to 29 cm yr^{-1}. Biomass and leaf area index heterogeneity predominantly controlled this complexity, while biophysical differences between deciduous and coniferous vegetation were of secondary importance. Spatial aggregation of land cover characteristics resulted in mean monthly NPP estimation bias from 25 to 48% (0.11–0.20 g C m^{-2} d^{-1}) and annual estimation errors from 2 to 14% (0.04–0.31 Mg C ha^{-1} yr^{-1}). Error was reduced at longer time intervals because coarse scale overestimation errors during spring were partially offset by underestimation of fine scale results during summer and winter. ET was relatively insensitive to land cover spatial scale with an average bias of less than 5% (0.04 kg m^{-2} d^{-1}). Factors responsible for differences in scaling behavior between ET and NPP included compensating errors for ET calculations and boreal forest spatial and temporal NPP complexity. Careful consideration of landscape spatial and temporal heterogeneity is necessary to identify and mitigate potential error sources when using plot scale information to understand regional scale patterns. Remote sensing data integrated within an ecological process model framework provides an efficient mechanism to evaluate scaling behavior, interpret patterns in coarse resolution data, and identify appropriate scales of operation for various processes.

1. Introduction

The boreal forest has received increasing attention from the scientific community in recent years because of its importance as a major reservoir of the world's carbon and mounting evidence that the magnitude and stability of this reservoir may be changing [e.g., *Chapin et al*., 1995; *Myneni et al*., 1997; *Goulden et al*., 1998]. The Boreal Ecosystem-Atmosphere Study (BOREAS) was an interdisciplinary field experiment designed to assess the magnitude and direction of boreal forest surface-atmosphere exchanges of energy, water, and carbon as well as the factors regulating these exchanges and their sensitivity to climate change [*Sellers et al*., 1997]. A key BOREAS objective has been to quantify these processes at local scales (i.e., <1 km^2) and to extrapolate results to regional scales consistent with atmospheric general circulation model (GCM) and other global data sets using process-type models driven by aircraft and satellite remote sensing inputs [*Sellers et al*., 1997].

GCMs and other regional scale models generally define surface-atmosphere conditions and fluxes at scales of 100 km^2 or more, where minimum grid cell sizes often represent area averages of highly heterogeneous surface features. The boreal forest, in particular, represents a complex land cover mosaic where vegetation morphology, condition, and distribution are strongly regulated by environmental factors such as moisture availability, growing season length, disturbance, and nutrient levels [*Bonan and Shugart*, 1989]. Flux rates and physiological responses to environmental controls within boreal forest communities have also been shown to be nonlinear, spatially variable, and strongly dependent on site conditions and stand physiological characteristics [e.g., *Bonan*, 1993; *Dang et al*., 1997a, *Hogg and Hurdle*, 1997]. Deciduous aspen stands, for example, exhibit larger carbon and water fluxes per unit leaf area than coniferous jack pine and black spruce stands under optimal conditions, though annual productivity for deciduous vegetation is limited by a shorter growing season [*Black et al*., 1996; *Baldocchi et al*., 1997a; *Goulden et al*., 1998]. Stomatal sensitivity to vapor pressure deficit (VPD) also tends to be greater for aspen stands than for jack pine and black spruce stands [*Dang et al*., 1997a].

Land cover features essential for characterizing regional fluxes may not be distinguished at coarse spatial resolutions. Wetlands, for example, represent less than 7% of the BOREAS southern study area (SSA) but may play a major role in the regional carbon balance [*Roulet et al*., 1997]. Accurate

Paper number 1999JD900085.
0148-0227/99/1999JD900085$09.00

distinctions between boreal needleleaf coniferous and broadleaf deciduous forest types have also been found to be critical for determining regional net photosynthesis [*Bonan*, 1993]. Unfortunately, these features may not be adequately represented at spatial scales consistent with regional data sets. A key issue in evaluating boreal forest ecological and physical processes at various scales is the influence of sub-grid-scale land cover features on regional water and carbon fluxes.

The purpose of this investigation is to evaluate the effect of boreal forest land cover heterogeneity on regional mean water and carbon flux simulations using a process level ecosystem model, BIOME-BGC, coupled with remote sensing derived parameter maps of key state variables at different spatial scales. We use remote sensing derived maps of land cover type, crown, and stem biomass as model inputs to determine regional mean evapotranspiration and net primary productivity within the BOREAS southern modeling subarea (SMSA). Model simulations are conducted using input data at length scales ranging from 30 to 50 km. These methods are used to assess the importance of sub-grid-scale land cover variability on regional biogeochemical processes over a 3 year period, from 1994 to 1996.

2. Background

Remote sensing provides a means for mapping state variables such as land cover type and leaf area that can be used within an ecological model framework to determine regional scale processes such as photosynthesis, respiration and evapotranspiration [e.g., *Sellers et al*., 1986; *Running and Gower*, 1991]. Two major factors affect the characterization of regional fluxes with this method: (1) the influence of sub-grid-scale processes within the aggregate and (2) the degree of nonlinearity between model inputs and outputs. Most process models employ similar sets of functional relationships that have generally been developed at the plot level where direct measurement and control of vegetation, soil, and meteorological conditions is possible. These methods accurately represent point level processes but ignore or greatly simplify the effects of spatial heterogeneity in the driving variables. As a result, models that utilize nonlinear, plot scale relationships may produce biased results when simple arithmetic means are used to describe complex surfaces at regional scales. The propagation of errors among the various functional relationships within the larger model framework may also be additive or compensatory depending on the specific process being modeled, model time step, and land surface characteristics [*Rastetter et al*., 1992; *Band*, 1993; *Pierce and Running*, 1995; *Sellers et al*., 1995].

Remote sensing data can be used within a process model framework to partition habitats in which variation of the driving processes is minimized. This provides a mechanism where nonlinear biophysical relationships can be evaluated with minimal bias. Ideally, the spatial complexity of the processes and the degree of nonlinearity in their response determine the degree of partitioning. In practice, however, the scale and extent of available data and the computational efficiency of the model limit the degree of partitioning. If a critical land cover characteristic is inadequately represented or not resolved at the resolution of the spatial data, then significant bias may occur at regional scales. The challenge of regional modeling is to characterize the important components of the surface without overwhelming model computations with unnecessary detail [*Rastetter et al*., 1992].

Ecological model sensitivity to spatial scale has been found to vary depending on surface conditions and the nature and temporal scale of the variable being estimated. For coniferous forests of the mountainous, western United States, soil moisture heterogeneity was found to be a major source of bias for area-averaged carbon and water fluxes, particularly under drying conditions [*Band*, 1993; *Pierce and Running*, 1995]. When both deciduous and coniferous vegetation types were considered, land cover heterogeneity was found to be a major source of bias for area-averaged annual carbon fluxes, while annual water fluxes were relatively insensitive to spatial scale [*Turner et al*., 1996]. For tallgrass prairie regions of the central United States, relationships describing the effects of moderate topography on surface energy and water fluxes were found to be near linear and largely scale invariant provided that the vegetation type was relatively homogenous [*Sellers*, 1992; *Sellers et al*., 1995].

The southern boreal forest is characterized by large seasonal variations in solar irradiance and temperature that generally limit the growing season to spring and summer months. Much of the annual precipitation falls during the growing season, though dry summer periods are known to occur and can be water limiting for ecosystem processes. The topography is gentle to moderate, while low solar elevation angles enhance topographic effects on microclimate. These factors combined with variable fire and other disturbance regimes create a complex mosaic of soil and vegetation characteristics that may not be adequately represented at spatial scales coarser than ~30 m [*Bonan and Shugart*, 1989]. Vegetation type and structure are important in regard to regional flux rates because physiological differences in assimilation rates, canopy conductances, carbon allocation, and nutrient use efficiencies strongly influence carbon and water exchanges with the atmosphere [*Bonan*, 1993; *Sellers et al*., 1995; *Dang et al*., 1997a, b]. At coarser spatial scales, sub-grid-scale land cover characteristics may exert a major control over regional mean water and carbon fluxes. These relationships may also vary as surface resistance characteristics change, in response to interannual variations in weather patterns.

3. Methods

3.1. Study Area Description

The focus of our investigation lies within the BOREAS SMSA, which covers an area of ~40 km by 50 km within central Saskatchewan, Canada (≅53°55′N, 104°48′W) and is fairly typical of the southern boreal forest region [*BOREAS Science Team*, 1995; *Sellers et al*., 1997]. Topographic variability is low with elevations ranging from 440 to 660 m and slopes generally less than 5%. Vegetation in the region is composed of both deciduous and coniferous life forms. Dry, sandy upland sites support jack pine (*Pinus banksiana*) stands, while aspen (*Populus tremuloides*), balsam poplar (*Populus balsamifera*), and white spruce (*Picea glauca*) species are found on well-drained, glacial deposits. In wet, poorly drained areas, black spruce (*Picea mariana*) and tamarack (*Larix laricina*) species are common. Bogs and fens are also common in poorly drained areas and are mainly composed of sedges (*Carex spp*.) interspersed with black spruce, tamarack, and bog birch (*Betula pumila*) species. Logging and fire-related disturbances also play a major role in shaping vegetation patterns in the area. Localized logging for paper pulp and fence posts is common along roadside areas within the study area, while the northeast portion of the SMSA encompasses part of an extensive burn,

which occurred in 1977 and 1978. This area is predominantly covered with small (<5 m) jack pine regrowth. Additional fires and logging activity occurred in 1995 and 1996. However, changes in land cover characteristics after 1994 were not addressed in this investigation.

3.2. Ecosystem Model Description

BIOME-BGC (BioGeoChemistry) is a process-level, ecosystem model that simulates biogeochemical and hydrologic variables within multiple biomes. Model logic is based on the assumption that differences in process rates among biomes are primarily a function of climate and general life-form characteristics [*Running and Hunt*, 1993]. The model represents a compromise between (1) the desire to represent detailed surface structure and biophysical interactions readily observed at the plot scale and (2) the limitations of surface biophysical, meteorological, and validation information at regional scales. The model employs several simplifying strategies regarding stand and meteorological conditions to facilitate application at regional scales. The surface is represented by singular, homogeneous canopy and soil layers where understory processes are not distinguished from the aggregate. Meteorological characteristics are defined from daily minimum and maximum air temperature, precipitation, and solar irradiance. These data are used in conjunction with general stand and soil information to predict net photosynthesis, respiration, evapotranspiration, snow cover, and soil water conditions on a daily basis. BIOME-BGC logic, input requirements, and model applications for various environments are well documented elsewhere [e.g., *Hunt and Running*, 1992; *Running and Hunt*, 1993; *Hunt et al*., 1996]. Documentation of model structure and input requirements unique to the BOREAS environment are also provided by *Kimball et al*. [1997a, b]; these results compared favorably with 1994 tower flux and hydrologic measurements over various stands within the study region. A summary of model structure relating to the characterization of spatially distributed carbon and water fluxes within the SMSA is provided here.

Net primary production (NPP) represents the net accumulation of carbon by the stand and is determined as the daily difference between gross photosynthesis and respiration from maintenance (R_m) and growth (R_g) processes. Photosynthesis is calculated using a modified form of the Farquhar biochemical model [*Farquhar and von Caemmerer*, 1982; *Kimball et al*., 1997a]. Photosynthetic response is regulated by canopy conductance to CO_2, leaf maintenance respiration, and daily meteorological conditions including air pressure, air temperature, and solar irradiance. Canopy CO_2 conductance is calculated as a proportion (62.5%) of the canopy conductance to water vapor (g_c). The maximum canopy water vapor conductance ($g_{c,\max}$) defines the upper boundary of the photosynthetic rate and is determined by leaf area index (LAI) and prescribed leaf scale boundary layer (g_{bl}) and stomatal minimum ($g_{st,\min}$) and maximum ($g_{st,\max}$) conductances to water vapor; g_c is reduced in a nonlinear fashion when air temperature (T_a), VPD, solar irradiance, or soil water potential (PSI) deviate from prescribed optimal conditions [*Running and Hunt*, 1993; *Kimball et al*., 1997a].

R_m represents the total loss of carbon from the system due to day and night leaf respiration ($R_{dl} + R_{nl}$), sapwood (R_{sw}), coarse root (R_{cr}), and fine root (R_{fr}) respiration components. R_m is calculated from mean daily air temperatures and prescribed foliar, root (coarse plus fine) and stem carbon pools using an exponential relationship between respiration and temperature [*Kimball et al*., 1997a]. The magnitude of the respiration response to temperature is governed by a prescribed rate defined at a reference temperature (i.e., 20°C) and a proportional rate change for a 10°C change in temperature (Q_{10}). Daily growth respiration was not determined explicitly by the model but was computed as a proportion (32%) of the daily difference between gross photosynthesis and R_m [*Penning and de Vries*, 1974; *Lavigne and Ryan*, 1997].

Evapotranspiration is computed as the daily sum of transpiration and evaporation from surface, snow, and canopy components. Both transpiration and evaporation components are estimated from daily air temperature, humidity, and solar irradiance information using a modified Penman-Monteith approach [*Running and Hunt*, 1993; *Kimball et al*., 1997b]. Maximum transpiration rates are regulated by g_c. Maximum surface evaporation rates are controlled by a surface conductance term that deviates from an optimal rate using an inverse exponential decay function based on the number of days since a rainfall event [*Kimball et al*., 1997b].

Since its inception as a point scale model, BIOME-BGC has evolved to simulate regional scale processes by incorporating spatially distributed daily meteorological fields derived from a microclimate simulator, and remote sensing derived surface parameter maps to define important landscape characteristics. The model employs a biome-level stratification of land cover conditions to minimize spatial variability in conversion efficiencies and potential environmental controls. The model is now capable of simulating ecosystem processes over landscapes ranging from watershed to global scales [*Running et al*., 1989; *Running and Hunt*, 1993; *Hunt et al*., 1996].

3.3. Ecosystem Model Inputs and Initialization

3.3.1. Biophysical constants. For landscape simulations, BIOME-BGC uses a spatial database composed of soil, vegetation, and daily meteorological characteristics registered to a common projection format, as well as array of critical physiological constants that define the environmental response curves of individual biome types within the spatial domain (see Table 1). These physiological constants were obtained from BOREAS field measurements when possible. When these data were unavailable, values were selected from the literature for representative cover types under similar environmental conditions.

3.3.2. Remote sensing inputs. Remote-sensing-derived crown and stem biomass and land cover classification maps were used to drive model simulations within the SMSA. Crown and stem biomass maps were derived from 1994 airborne synthetic aperture radar (AIRSAR) remote sensing measurements of the SMSA from a DC-8 aircraft [*BOREAS Science Team*, 1995; *Saatchi and Moghaddam*, 1999a, b]. Land cover classification maps were obtained at 30 m and 1 km spatial resolutions from AIRSAR and NOAA AVHRR sensor information collected during the 1994 growing season over the SMSA [*Saatchi and Rignot*, 1997; *Steyaert et al*., 1997]. The spatial extent of the AIRSAR-derived land cover and biomass maps defined the study area for this investigation, which was limited to ~1205 km^2 within the SMSA (see Figure 1).

Land cover classification maps were used to define the number of individual biome types represented in the ecosystem model, while biomass maps were used to define LAI and foliar and stem carbon pools within each grid cell. The AIRSAR classification map was used to characterize land cover over the 30 m spatial grid, while the AVHRR classification map defined

Table 1. Summary of BIOME-BGC Constants for Coniferous and Deciduous Vegetation Types Within the BOREAS SMSA

Parameter	Coniferous	Deciduous	Reference
Leaf N in Rubisco, %	6.0	14.0	1, 2
Max g_s, mm s^{-1}	1.0	7.0–8.0	3, 4
g_{bl}, mm s^{-1}	0.3	0.3–0.4	5
Optimal air temperature for g_s, °C	15.0	15.0	6, 11
PSI at stomatal closure, −MPa	2.5–4.0	2.0–4.0	3
VPD at stomatal closure, kPa	1.6–2.75	1.75	3, 4
Albedo (no snow conditions, %)	10.0	20.0	8
Leaf, fine root R_m proportions at 20°C, 1/day	0.002	0.009	7, 9, 10
Stem, coarse root R_m proportions at 20°C, 1/day	0.001	0.004	7, 9, 10
Canopy extinction of PAR	−0.5	−0.5	5, 12
Q_{10} for R_m	2.0	2.0	7
Ratio of total to projected LAI	2.2	2.0	5, 7
SLA (1-sided), m^2 kg^{-1} C^{-1}	6.0	22.5	12

Constants were estimated from both BOREAS field measurements and literature sources for representative cover types. 1, *Field and Mooney* [1986]; 2, *Fan et al*. [1995]; 3, *Dang et al*. [1997a]; 4, *Hogg and Hurdle* [1997]; 5, *Waring and Running* [1998]; 6, *Baldocchi et al*. [1997a]; 7, *Sprugel et al*. [1995]; 8, *Betts and Ball*. [1997]; 9, *Vowinckel et al*. [1975]; 10, *Johnson-Flanagan and Owens* [1986]; 11, *Lavigne and Ryan* [1997]; 12, *Dang et al*. [1997b].

land cover characteristics at the 1 km spatial scale. The classification maps were used to distinguish seven land cover classes within the SMSA, representing dry conifer (DC), wet conifer (WC), open water (OW), disturbed (DSTRB), deciduous (DEC), mixed deciduous/conifer (MX), and wetland (WD) areas. DC areas were mainly composed of jack pine stands, while WC areas consisted mainly of black spruce stands. WD areas were composed of a mixture of black spruce, bog, and fen sites, while DSTRB sites represented a mixture of recently logged or burned areas, roads, and other sparsely vegetated and nonwater surfaces. DEC areas were generally composed of greater than 80% deciduous cover dominated by aspen stands and grassland. MX areas represented a mixture of mainly jack pine and aspen forest with no clear dominance of either species type.

Our analysis focused on vegetated cover within the study area only. Open water areas were not represented in the model and were masked from further analysis. Deciduous and conif-

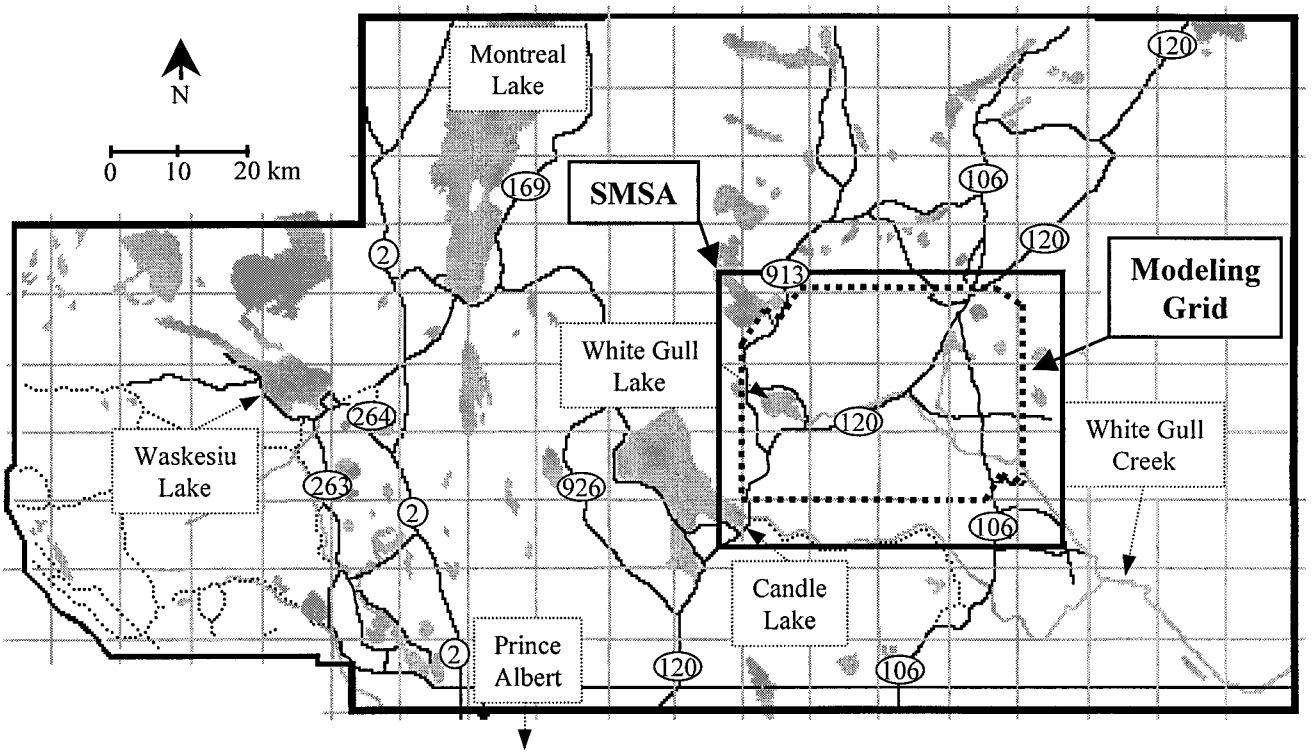

Figure 1. Map of the BOREAS southern study area (SSA). The study region (i.e., modeling grid) for this investigation (enclosed by the dashed line) represented an area of ~1205 km^2 within the BOREAS southern modeling subarea (SMSA) and was defined by the spatial extent of available AIRSAR-derived biomass and land cover information.

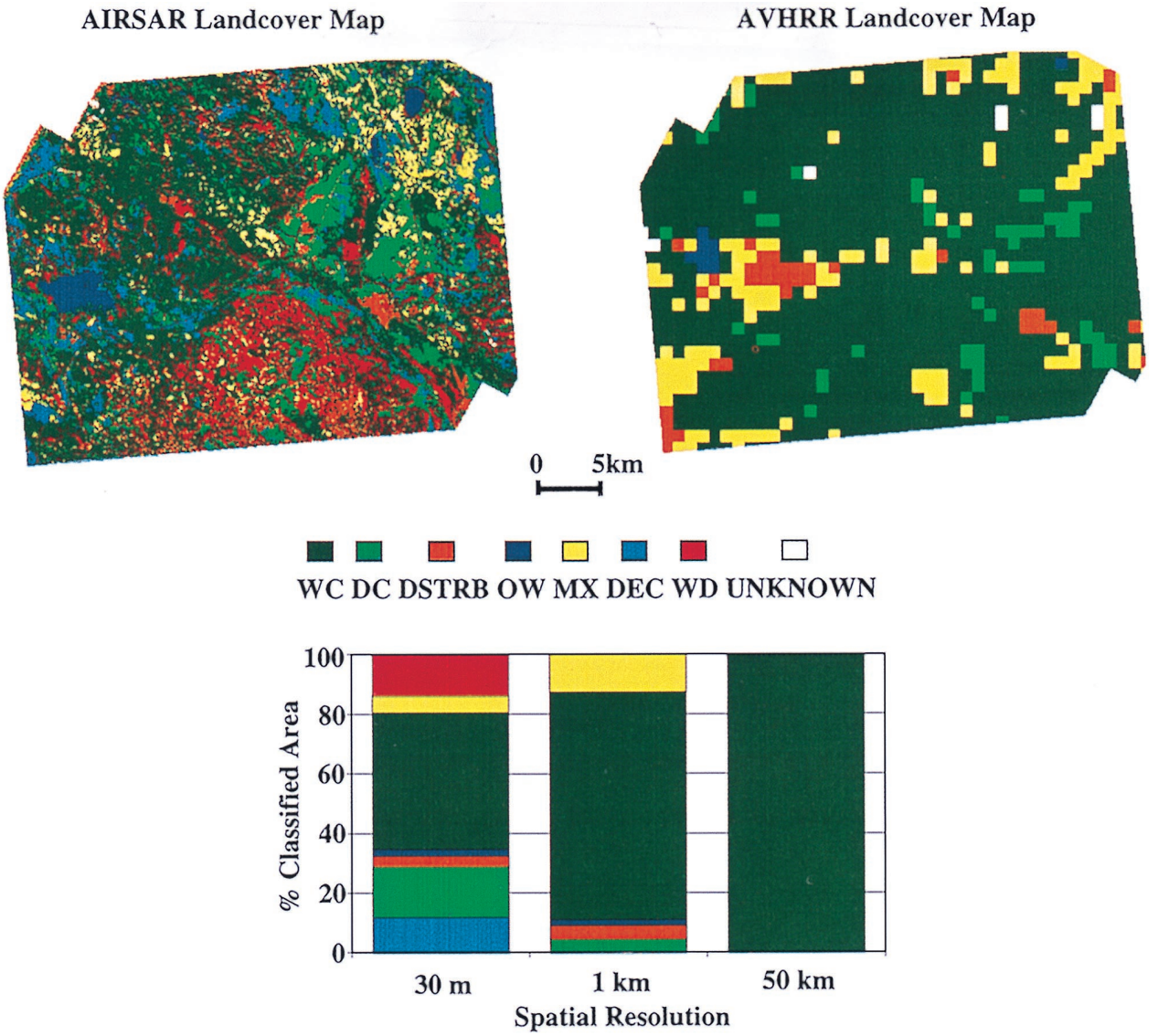

Plate 1. Land cover classification maps of the study area at 30 m and 1 km spatial scales; the images are in the BOREAS grid system [*BOREAS Science Team*, 1995] which is an Albers equal-area conic projection. The bottom graph shows the proportion of classified area represented by each land cover class at 30 m, 1 km, and 50 km spatial scales.

erous canopies within mixed cells were simulated separately because of marked differences in biophysical characteristics and physiological responses to environmental controls. DC and WC classes were assumed to be composed entirely of coniferous vegetation, while DEC areas were assumed to be 100% deciduous. DSTRB, MX, and WD classes were represented as a mixture of 50% deciduous and 50% coniferous life-forms. Ideally, information on deciduous and coniferous proportional cover characteristics could be used to simulate the relative contributions of these life-forms to the total water and carbon flux within each cell. Unfortunately, this information was not available for the investigation, so simplifying assumptions were necessary.

3.3.3. Derived inputs. The mass of living stem carbon was derived from the stem biomass map and estimates of the relative proportions of living and total stem biomass, and the proportions of living cells in sapwood tissue. This information was obtained from biomass harvest plots within the SSA and information reported in the literature for representative vegetation types [*Gower et al*., 1997; *Waring and Running*, 1998]. The mass of living coarse root carbon was estimated as a proportion (0–25%) of live stem carbon using allometric relationships for representative cover types [*Grier et al*., 1981; *Vogt*, 1991; *Steele et al*., 1997]. The mass of living fine root carbon was estimated from 1.5 to 3.0 times foliar carbon estimates based on SSA biomass measurements and information reported in the literature for nutrient limited arctic, boreal, and cold temperate environments [*Bigger and Oechel*, 1982; *Mitsch and Gosselink*, 1993; *Schimel et al*., 1996; *Gower et al*., 1997; *Steele et al*., 1997].

The mass of foliar carbon was derived from AIRSAR crown biomass (i.e., leaves plus branches) maps and estimated proportions of foliar to crown biomass obtained from biomass harvest plots within the SSA [*Gower et al*., 1997]. LAI was derived from foliar carbon maps and specific leaf area (SLA)

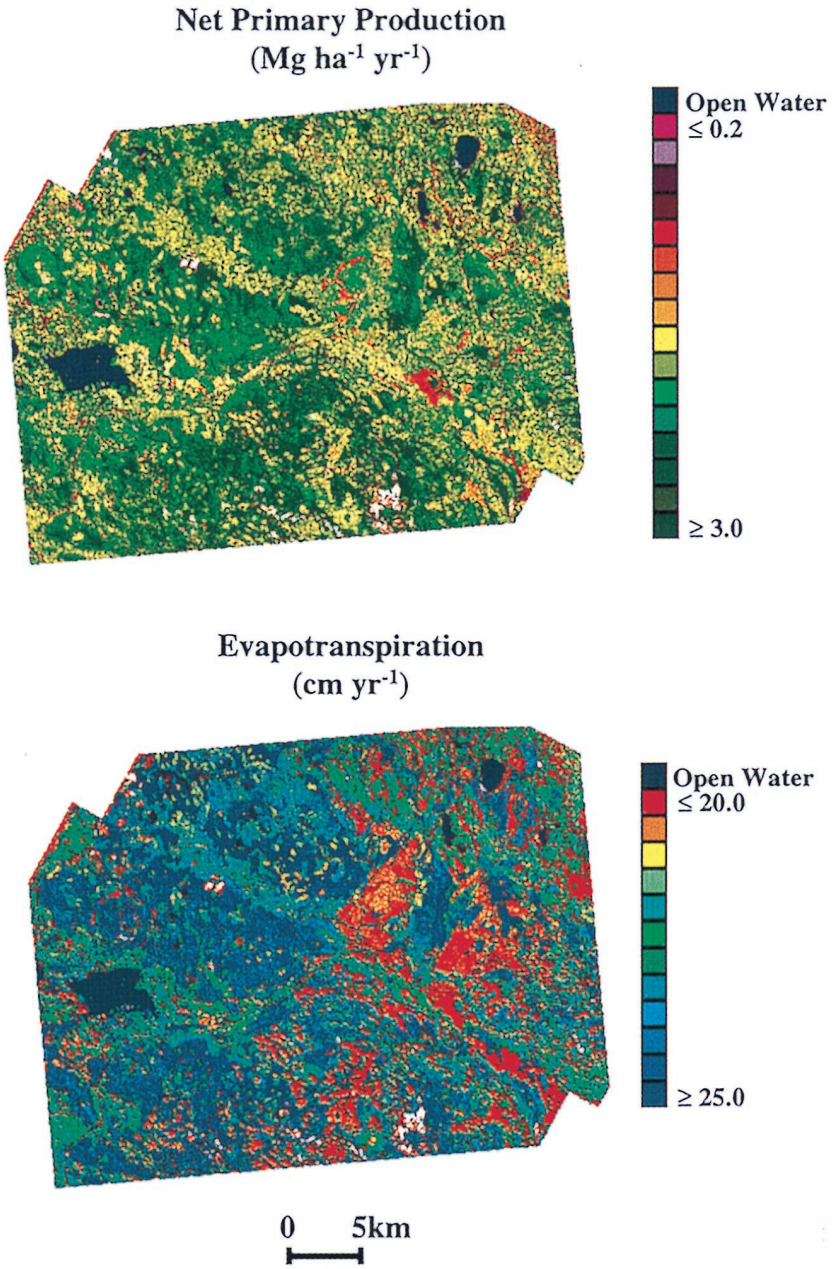

Plate 2. Year 1994 simulated annual NPP (Mg C ha^{-1} yr^{-1}) and ET (cm yr^{-1}) within the BOREAS SMSA study area using BIOME-BGC and a 30 m land cover database; the images are in the BOREAS grid system [*BOREAS Science Team*, 1995] which is an Albers equal-area conic projection. The SMSA covers an area ~40 km by 50 km, while the size of the study area is slightly smaller and was defined by the aerial extent of available AIRSAR remote sensing data. White areas represent unknown surface land cover conditions that were masked from model analysis.

values obtained from canopy biophysical measurements within the SSA [*Dang et al*., 1997b]. The LAI for coniferous vegetation was held constant over each year. For deciduous vegetation, LAI was regulated between a prescribed seasonal minimum (i.e., 0.0) and the remote sensing defined seasonal maximum using a phenology model based on daily meteorological predictions of satellite-observed dates of greenness onset and offset [*White et al*., 1997]. The model predicts the onset of greenness using a combined thermal and radiation summation, while offset is determined using a thermally adjusted photoperiod trigger. The foliar carbon pool was increased on a daily basis using a stepped, 45-day linear ramping function between the onset date and the AIRSAR defined LAI, while foliage drop occurred at the offset date.

Foliar leaf nitrogen concentrations (N_{leaf}) strongly influence the photosynthetic capacity of the system and are directly related to the amount of radiation absorbed by the canopy [*Schimel et al*., 1991; *Pierce et al*., 1994]. Because canopy absorption is also related to LAI, N_{leaf} was estimated as a proportion (0.7–4.5%) of leaf biomass. These fractions were derived from site measurements within BOREAS aspen, jack pine, and black spruce stands [*Dang et al*., 1997b; *Sullivan et al*.,

Table 2. Weather Summary for the Nipawin Airport Weather Station (≈53°20′N 104°00′W) Located Near the SE Corner of the SMSA

Characteristic	1994	1995	1996	1976–1997	$s.d._{1976-1997}$
Mean air temperature, °C	0.60	0.24	−1.24	0.76	1.13
Mean air temperature, °C, fall	3.39	1.15	−0.24	1.80	1.67
Mean air temperature, °C, spring	3.5	−0.46	−1.51	1.59	1.93
Mean air temperature, °C, summer	15.78	16.65	17.13	16.39	1.19
Total precipitation, cm	45.56	42.52	49.76	44.28	6.01
Total rainfall, cm	39.84	30.16	38.12	34.99	6.08
Total snow water equivalent, cm	5.72	12.36	11.64	9.29	2.46

Data represent mean annual weather conditions for 1994–1996, as well as long-term (1976–1997) means and standard deviations (s.d.) for the site; air temperature data are also summarized for fall (September 1 to November 30), spring (March 1 to May 31), and summer (June 1 to August 31) conditions.

1997] and values reported in the literature for representative cover types [*Aerts et al*., 1992; *Mitsch and Gosselink*, 1993; *Schimel et al*., 1996].

Soil-rooting depth and water-holding capacity information were derived for each land cover class from a $1:10^6$ scale digital soils inventory database of Canada [*Acton et al*., 1991], as well as volumetric soil moisture and soil survey measurements conducted at several sites within and adjacent to the SMSA [*Boreas Science Team*, 1995; *Cuenca et al*., 1997]. Soil *b*-parameter values define the slope of the functional PSI response to changes in soil water and were derived from values reported in the literature for representative soil types [*Cosby et al*., 1984]. For this investigation, soil structural characteristics were defined for each land cover type and assumed constant within the area represented by each land cover class at each spatial scale.

3.3.4. Meteorological inputs. BIOME-BGC uses daily maximum and minimum air temperatures, solar irradiance (direct plus diffuse), and precipitation to determine daily carbon and water fluxes. Daily meteorological data were interpolated over a 1 km resolution, digital elevation map (DEM) of the SMSA using a daily meteorological interpolator [*Running et al*., 1989; *Thornton et al*., 1997], digital elevation information (i.e., elevation, slope, aspect), and daily meteorological data from ~60 weather stations within the BOREAS region. Gridded daily meteorological data were produced for the 3 year (1994–1996) study period. Meteorological data were obtained from the National Climatic Data Center's Global Surface Summary of the Day database, the Saskatchewan Research Council's Automatic Meteorological Stations database, and BOREAS tower flux site measurements within the SSA [*National Weather Service*, 1988; *Boreas Science Team*, 1995; *Shewchuk*, 1997]. DEM information were provided by the BOREAS HYD-08 team and BOREAS staff [*BOREAS Science Team*, 1995].

Daily model simulations were conducted within the study region from January 1, 1994 to December 31, 1996. Meteorological conditions were defined using the 3 year gridded daily meteorological fields, while 1994 land cover type and biomass maps defined surface physical conditions for the three 3 year period. Spatially distributed estimates of initial soil water and snow water equivalent depth were required to initialize the 1994 water balance. The model was initialized with a uniform, snow water equivalent depth of 3.3 cm and a soil water content set at 95% of field capacity. These values were determined from BIOME-BGC point simulations at BOREAS SSA tower sites using 1993 daily meteorological data from Nipawin Airport (≈53°20′N 104°00′W) near the SE corner of the SMSA.

3.4. Model Output Analysis

The goal of this investigation is to test the sensitivity of regional NPP and evapotranspiration simulations to the spatial scale of input land cover type and vegetation structural conditions within the SMSA. BIOME-BGC was run using 1 km DEM and gridded meteorological information with land cover, crown, and stem biomass data assembled at 30 m, 1 km, and 50 km spatial scales. These minimum cell sizes are generally consistent with the variety of satellite sensor information available for the region, including Landsat TM, NOAA AVHRR, and global scale land cover data sets [e.g., *Steyaert et al*., 1997]. Crown and stem biomass data were aggregated to 1 and 50 km spatial grids using an averaging window of 30 m resolution cells. AIRSAR and TM classification maps defined land cover characteristics at the 30 m resolution, while the AVHRR classification map defined the number of land cover classes at the 1 km resolution. Land cover was determined at the 50 km

Table 3. Statistical Summary (Means With Standard Deviations in Parentheses) of Crown and Stem Biomass (kg m^{-2}), Leaf Area Index (LAI, 1-sided), Foliar and Live Stem Carbon (kg m^{-2}) for Wetland (WD), Mixed Forest (MX), Dry Conifer (DC), Wet Conifer (WC), Disturbed (DSTRB), and Deciduous (DEC) Landcover Types Within the SMSA

Parameter	WD	MX	DC	WC	DSTRB	DEC	Total
Crown B	1.5 (0.3)	2.1 (0.2)	1.2 (0.2)	1.8 (0.3)	0.3 (0.2)	1.5 (0.2)	1.6 (0.36)
Stem B	7.1 (1.6)	8.7 (0.8)	5.2 (1.7)	7.0 (2.0)	0.0	11.7 (1.7)	7.4 (2.6)
LAI	3.3 (0.6)	4.5 (0.4)	2.5 (0.3)	4.3 (0.8)	0.6 (0.4)	3.3 (0.4)	3.7 (0.9)
Foliar C	0.3 (0.06)	0.5 (0.04)	0.4 (0.05)	0.7 (0.13)	0.1 (0.04)	0.2 (0.01)	0.5 (0.23)
Stem C	0.2 (0.04)	0.3 (0.03)	0.1 (0.02)	0.2 (0.03)	0.04 (0.03)	0.03 (0.03)	0.2 (0.05)

Biomass data were obtained directly from AIRSAR 30 m remote sensing data, while the other variables were derived indirectly from the biomass maps, surface biophysical and biomass measurements.

resolution by selecting the dominant cover class (i.e., mode) from a histogram of the 1 km land cover classification data for the study area.

Bias was assessed between spatially averaged monthly and annual means of daily NPP and ET results for each of the three years of the investigation. Model output bias was determined as the absolute difference between 30 m (i.e., base conditions) and coarser resolution results and then summarized as a percentage of the mean annual base value. At monthly timescales the correspondence between base conditions (dependent variable) and aggregated (independent variable) results was assessed using linear regression analysis, while significance ($p < 0.05$) of the differences in monthly and annual results was evaluated using a student's *t*-test.

4. Results and Discussion

4.1. Regional Meteorological Characteristics

Meteorological conditions from 1994 to 1996 were quite different relative to the long-term (22 years) record for the region (see Table 2). The year 1994 had relatively warm spring and fall conditions, with a cooler summer and more precipitation than normal; 1995 and 1996 generally had cooler spring and fall conditions but warmer summer temperatures than 1994 or the long-term record. Summer conditions for 1995, however, were drier than 1994, 1996, or the long-term record.

Spatial variability in gridded air temperature and solar irradiance represented less than 6% (0.3°C) and 0.9% (1.5 W m^{-2}) of mean annual results, respectively. The gentle topography of the SSA and similar daily meteorological conditions for weather stations in and around the study region were generally responsible for the low spatial heterogeneity in these results. Spatial variability in annual precipitation was also low, representing less than 7% (0.4 cm) of the mean annual total precipitation for the region. However, variability in daily precipitation was much greater due to the predominance of small, spatially erratic precipitation events produced by convective activity during the summer months. Spatial heterogeneity in daily meteorological conditions were likely much greater than our results indicate due to the influence sub-grid-scale microtopography, vegetation, and moisture effects on the surface energy balance. These effects may influence regional water and carbon fluxes but were not addressed within the framework of this investigation because of the coarse nature of the DEM and the low surface station density (~<1 station per 1900 km^2).

4.2. Aggregation Effects on Land Cover Characteristics

Seven land cover classes were distinguished using the 30 m, land cover map (see Plate 1). WC was the dominant cover class, representing 45.9% of the study area. Other classes represented from 2.2% (OW) to 17.1% (DC) of the region and were generally more dispersed and fragmented than WC areas. At the 1 km resolution, WC and MX were the dominant cover classes, representing 76.5 and 12.5% of the region, respectively. WD and DEC cover classes were no longer distinguished, while DC, DSTRB, and OW classes each represented less than 5% of the study area. Wetlands, small water bodies, and small DC stands identified at the 30 m scale were generally merged into the WC class, while mixed forest and deciduous stands were merged into both the MX and the DSTRB classes. These results are consistent with land cover map comparisons using Landsat TM and NOAA AVHRR information for the BOREAS SSA [*Hall et al*., 1997; *Steyaert et al*., 1997]. As the spatial grid was aggregated to 50 km, the proportional area represented by the dominant WC class grew to represent 100% of the study region; this is also consistent with other land cover representations of the region derived from global data sets [e.g., *Matthews*, 1983; *Steyaert et al*., 1997].

Remotely sensed biomass and derived LAI, foliar, and stem carbon distributions were quite variable over the 30 m spatial grid, both within and between different land cover classes (see Table 3). These results were generally consistent with the ranges of values reported by other investigators using allometric relationships, biomass and optical LAI field measurements, as well as satellite-based optical and synthetic aperture radar remote sensing of biomass within the BOREAS region [e.g., *Chen et al*., 1997; *Gower et al*., 1997; *Hall et al*., 1997; *Ranson et al*., 1997; *Saatchi and Moghaddam*, 1999a, b]. *Gower et al*. [1997], for example, estimated overstory LAI (projected) values of the order of 5.6 (±1.7), 2.8 (±0.8), and 3.3 (±0.7) for mature black spruce, jack pine, and aspen stands using biomass harvest plot information and allometric relationships within the BOREAS SSA. These values are similar in relative magnitude and range to AIRSAR-derived LAI for WC, DC, and DEC cover classes (Table 3).

Distributions of the AIRSAR-derived variables were normally distributed and significantly different ($p < 0.001$) between land cover classes. Within-class biomass diversity was large, however, with mean coefficients of variation ranging from 9% (MX) to 69 (DSTRB) %. Deciduous stands generally had the most aboveground biomass, though wet conifer stands tended to have the most crown biomass and leaf area. Disturbed sites had the lowest biomass and leaf area of all the classes due to the sparsely vegetated logged and burned conditions. Biomass levels within WD areas were generally intermediate between DC and WC classes. These levels are generally in the upper range of biomass values reported for Siberian and western European wetlands but are similar to values reported for forested fens, bogs, and peatlands in northern Minnesota and Michigan [*Mitsch and Gosselink*, 1993].

As the biomass maps were aggregated from 30 m to 1 km, variability in LAI and foliar C decreased by 13%, while stem C variability decreased by 17.0%. Population means were within 3% of the 30 m results regardless of spatial resolution, while the distributions of the variables tended to remain approximately normally distributed.

4.3. Ecosystem Model Results

Annual NPP and ET simulations exhibited a large degree of spatial variability at the 30 m scale (see Plate 2), ranging from ~0.1–3.9 Mg C ha^{-1} and 13–29 cm for 1994. Annual ET spatial patterns were directly related to the amount of surface biomass, particularly LAI, while NPP spatial patterns were related to both the LAI and the proportions of deciduous and coniferous vegetation. These results were normally distributed and were significantly different among the six land cover types ($p < 0.001$). Within-class variability was also substantial, with NPP and ET coefficients of variation of ~24% (±0.34 Mg C ha^{-1}) and 5% (±1.1 cm) for the 3 year period (see Table 4). Years 1995 and 1996 showed significant reductions in regional NPP of ~19% (0.4 Mg C ha^{-1}) due to cooler spring and warmer, drier summer conditions relative to 1994. Annual variations in ET were generally mixed. Overall, ET showed regional increases of 0.4% (0.1 cm) and 3.6% (0.8 cm) for 1995 and 1996, respectively. However, WD, DC, DSTRB, and DEC classes showed approximate 4% (0.8 cm) reductions in ET for 1995.

Simulated ranges and land cover differences in NPP were similar to observations reported by other BOREAS investigators using aboveground and below-ground biomass measurements and allometric relationships within black spruce, jack pine (young and mature), and aspen stands [*Gower et al*., 1997; *Steele et al*., 1997]. NPP observation data for fen and other wetland areas were not available within the SMSA. However, model results were similar to the magnitudes and ranges of NPP (aboveground only) reported in the literature for northern bog marshes, rich fen, forested peatland, and fen forest sites within Canada and the northern United States; reported values ranged from 0.5 to 9.7 Mg C ha^{-1} yr^{-1} [*Mitsch and Gosselink*, 1993].

The magnitudes and relative differences in ET between land cover classes were similar to 1994 cumulative ET estimates obtained from tower eddy-flux measurements at SSA black spruce [*Jarvis et al*., 1997], jack pine [*Baldocchi et al*., 1997b], and aspen (overstory) sites [*Black et al*., 1996]. Detailed comparisons were previously conducted between BIOME-BGC daily site simulations and tower eddy-flux and soil moisture measurements within the SSA for 1994 [*Kimball et al*., 1994b]. Model results explained 62 and 98% of the respective variances in observed daily evapotranspiration and soil water. Simulations of the onset of spring thaw and the dates of snowpack disappearance and accumulation were also generally consistent with observations [*Kimball et al*., 1997b].

4.4. Land Cover Aggregation Effects on NPP and ET Simulations

Monthly NPP bias averaged ~38% over the 3 year study period and corresponded to respective mean monthly differences of 0.13 and 0.19 g C m^{-2} d^{-1} at 1 and 50 km spatial scales (see Figure 2). For the 1994–1996 study period, 1 and 50 km results accounted for 94% (SE = 0.16 g C m^{-2} d^{-1}) and 90% (SE = 0.24 g C m^{-2} d^{-1}) of the variation in base conditions. Coarse resolution data generally resulted in spring overestimates and summer and winter underestimates of 30 m results. Differences between base and coarse resolution results were primarily due to canopy phenology and other biophysical differences between deciduous and coniferous life-forms. In 1994, estimated leaf-out for deciduous vegetation was initiated at the end of April and completed during the third week of June. This pattern is also consistent with 1994 observations within the SSA aspen tower flux site [*Black et al*., 1996]. In 1995 and 1996, spring conditions were much cooler, while simulated snow cover remained on the ground ~1 month longer than 1994. Snow depth measurements at the Nipawin atmospheric weather station (Table 2) also showed approximate 3 and 5 week delays in snow disappearance for 1995 and 1996, relative to 1994. Estimated leaf-out for these years did not occur until the last week of May and the first week of June, while deciduous canopies were not in full leaf until mid-July. As land cover conditions were aggregated from 30 m to 1 km and 50 km scales, the proportions of deciduous and coniferous vegetation represented within the study area decreased and increased, respectively (e.g., Plate 1). Underrepresentation of deciduous cover within the aggregate resulted in an overestimation of LAI and corresponding NPP fluxes during spring, prior to and during leaf-out of deciduous vegetation. Similarly, canopy foliar biomass and LAI were overestimated during winter months, resulting in overestimation of foliar respiration and corresponding underestimation of NPP.

Boreal forest deciduous stands are generally more productive than coniferous vegetation per unit leaf area under optimal conditions because of greater photosynthetic capacity and stomatal conductance characteristics (e.g., Table 1). During the summer months, coarse resolution data underestimated NPP relative to base conditions because the proportions of broadleaf deciduous vegetation were underrepresented, even though the mean LAI within the study area was relatively consistent at the various spatial scales.

Partial compensation of model errors between spring and summer and winter conditions resulted in a reduction of potential error at longer timescales. NPP annual error for 1994 was ~10.6 and 14.3% at 1 km and 50 km scales, respectively. These values corresponded to significant ($p < 0.001$) under-

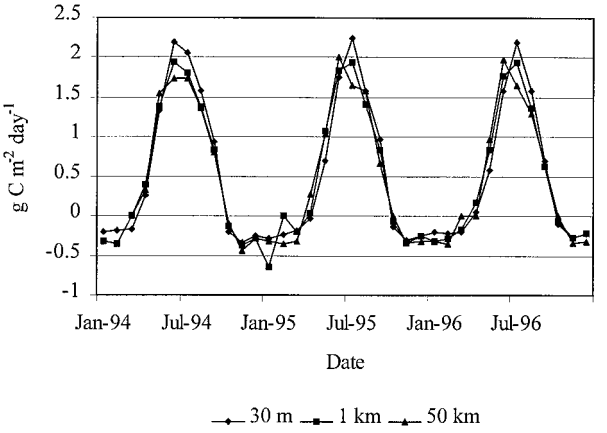

Figure 2. Plotted mean monthly integrated NPP (g C m^{-2} d^{-1}) derived from BIOME-BGC and land cover data at 30 m, 1 km, and 50 km spatial scales within the BOREAS SMSA study area. Significant reductions in model accuracy were reported on a monthly basis using 1 km ($r^2 = 0.94$, Std. Err. = 0.16 g C m^{-2} d^{-1}) and 50 km ($r^2 = 0.90$, Std. Err. = 0.24 g C m^{-2} d^{-1}) landcover data over the 1994–1996 study period. Annual bias was within 14.4% (0.31 Mg C ha^{-1} yr^{-1}) because coarse scale overestimation errors during spring were offset by underestimation of fine scale results during summer and winter.

Table 4. Annual Summary (Aerial Means With Standard Deviations in Parentheses) of BIOME-BGC Base Level (30 m) NPP and ET Simulations for Wetland, Mixed Forest, Dry Conifer, Wet Conifer, Disturbed, and Deciduous Landcover Types Within the SMSA

Cover Type	1994	1995	1996
	Total Net Primary Production, Mg C ha^{-1}		
WD	2.75 (0.39)	2.19 (0.34)	1.95 (0.32)
MX	3.37 (0.26)	2.74 (0.25)	2.50 (0.25)
DC	1.91 (0.27)	1.56 (0.23)	1.67 (0.24)
WC	2.05 (0.29)	1.89 (0.28)	1.84 (0.29)
DSTRB	1.0 (0.46)	0.88 (0.39)	0.80 (0.35)
DEC	1.95 (0.54)	1.06 (0.51)	0.72 (0.50)
Total	2.16 (0.56)	1.79 (0.53)	1.69 (0.55)
	Evapotranspiration, cm		
WD	23.32 (1.70)	23.04 (1.18)	23.90 (1.13)
MX	23.67 (1.71)	24.20 (0.93)	25.14 (0.99)
DC	21.39 (1.62)	19.61 (0.51)	20.51 (0.54)
WC	24.55 (2.07)	25.20 (1.99)	25.52 (2.12)
DSTRB	19.32 (0.25)	19.06 (0.21)	20.64 (0.35)
DEC	22.31 (0.73)	21.36 (0.63)	23.18 (0.65)
Total	23.12 (2.41)	23.20 (2.71)	23.96 (2.48)

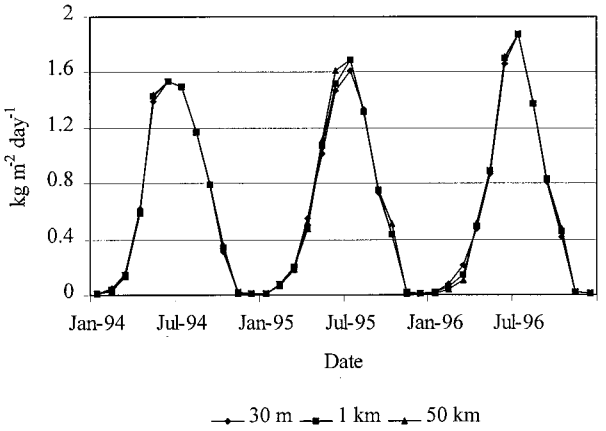

Figure 3. Plotted mean monthly integrated ET (kg m^{-2} d^{-1}) derived from BIOME-BGC and land cover data at 30 m, 1 km, and 50 km spatial scales within the BOREAS SMSA study area. Coarse resolution simulations generally agreed well ($r^2 = 0.97$, SE < 0.04 kg m^{-2} d^{-1}) with base level results over the 1994–1996 study period even though seasonal weather patterns were quite variable, ranging from cool spring, warm, dry (1995) and wet (1996) summer conditions, to warm spring and cool, wet summer (1994) conditions (see Table 2).

estimates of base level results of 0.23 and 0.31 Mg C ha^{-1} yr^{-1}. For 1995 and 1996, 1 and 50 km data resulted in small overestimates of base results, averaging 3.1% (0.06 Mg C ha^{-1} yr^{-1}) and 5.2% (0.09 Mg C ha^{-1} yr^{-1}), respectively.

Monthly bias for ET was much less than NPP, averaging 3.1% at 1 and 50 km scales and corresponding to errors of approximately 0.03 kg m^{-2} d^{-1} over the 3 year period (see Figure 3). Mean monthly ET derived from 1 km and 50 km data were not significantly different and also accounted for approximately 97% (SE < 0.04 kg m^{-2} d^{-1}) of the variance in 30 m results. The sensitivity of aerial average fluxes has been found to be generally greater under suboptimal conditions due to increased spatial heterogeneity in environmental controls and greater nonlinearity in system response curves [*Rastetter et al*., 1992; *Band*, 1993; *Sellers et al*., 1995]. Bias was generally greater during the 1995 and 1996 summer months because of warmer, drier conditions that resulted in greater spatial heterogeneity in surface resistances. On an annual basis, ET bias averaged 0.3% (0.1 cm yr^{-1}) for 1994 and 1.3% (0.3 cm yr^{-1}) for 1995 and 1996.

LAI accounted for 47–62% of the variance in annual NPP and 79–85% of the variance in annual ET for different land cover classes under base conditions for the 3 year study period (see Plate 3). *Bonan* [1993] found similar correspondences between LAI and net canopy assimilation of CO_2 for 21 black spruce, white spruce, aspen, balsam poplar, and paper birch stands near Fairbanks, Alaska. Much of the unexplained variance in NPP was due to phenological differences between deciduous and coniferous lifeforms. Reductions in the height and slope of the NPP, and LAI relationships for 1995 and 1996 were due to approximate 19% reductions in annual productivity associated with cooler spring temperatures and simulated 3–4 week delays in leaf-out of deciduous vegetation. Correspondences between 30 m LAI and NPP and ET results were also reduced for 1995 and 1996 because of greater spatial and temporal complexity in the response curves of different land cover types to warmer, drier summer conditions for these years.

Several factors contributed to partial reductions in model bias and observed differences in response between ET and NPP at coarse spatial scales. Land cover aggregation from 30 m to 50 km corresponded with reductions in biomass heterogeneity and extremes, as well as representation of both high and low productivity sites within the aggregate. The resulting impacts on mean errors from overestimation of NPP and ET in one area were partially balanced by underestimation of fluxes elsewhere. Mean ET fluxes between deciduous and coniferous life-forms also exhibited similar characteristics on a monthly and annual basis even though daily fluxes were generally quite different (e.g., Table 4) [*Kimball et al*., 1997b]. While broadleaf deciduous stands are generally capable of larger daily fluxes (per unit leaf area) under optimal conditions, WC and DC stands are less sensitive to adverse conditions such as high VPD and low soil moisture [e.g., *Dang et al*., 1997a]. Underestimation of ET due to underrepresentation of deciduous vegetation at coarse spatial scales was partially balanced by overestimation errors during suboptimal conditions and partial error compensation at longer timescales.

Another factor responsible for reduced ET sensitivity to land cover spatial scale is due to model interactions among LAI, transpiration, and evaporation. NPP, transpiration, and canopy evaporation (for boreal stands) show a direct linear response to LAI under optimal conditions. However, litter and soil surface evaporation show an apparent inverse response to LAI, because greater leaf area increases canopy interception of radiation, reducing energy available for surface evaporation [*Kimball et al*., 1997b; *Pierce and Running*, 1995]. This partial compensation of model error results in a relative reduction of ET (i.e., transpiration plus litter and soil evaporation) sensitivity to LAI spatial heterogeneity within the aggregate.

5. Summary and Conclusions

The purpose of this investigation was to evaluate the sensitivity of regional means of monthly and annual ET and NPP simulations to boreal forest, sub-grid-scale land cover complexity. Sensitivity was assessed over a 3 year period (1994–1996), ranging from warm spring and cool, moist summer conditions to cool spring and warm, dry summer conditions. Our results show that NPP is strongly sensitive to land cover heterogeneity, particularly in regard to the relative proportions of deciduous and coniferous vegetation represented within the aggregate. Inadequate representation of these differences at regional scales resulted in mean monthly bias from 25 to 48% (0.11–0.20 g C m^{-2} d^{-1}). However, error was reduced to 2.4–14.3% (0.04–0.31 Mg C ha^{-1} yr^{-1}) at annual time intervals because coarse scale overestimation errors during spring were partially balanced by underestimation errors during summer and winter. ET was relatively insensitive to land cover spatial scale, with monthly bias averaging less than 5% (0.04 kg m^{-2} d^{-1}). Several factors were responsible for differences in scaling behavior between ET and NPP, including compensating errors for ET calculations and boreal forest spatial and temporal NPP complexity.

NPP and ET sensitivity to land cover spatial scale was also found to vary depending on year-to-year fluctuations in weather patterns. Variations in the timing of seasonal thaw and growing season length, as well as suboptimal air temperature and moisture conditions during the growing season, were

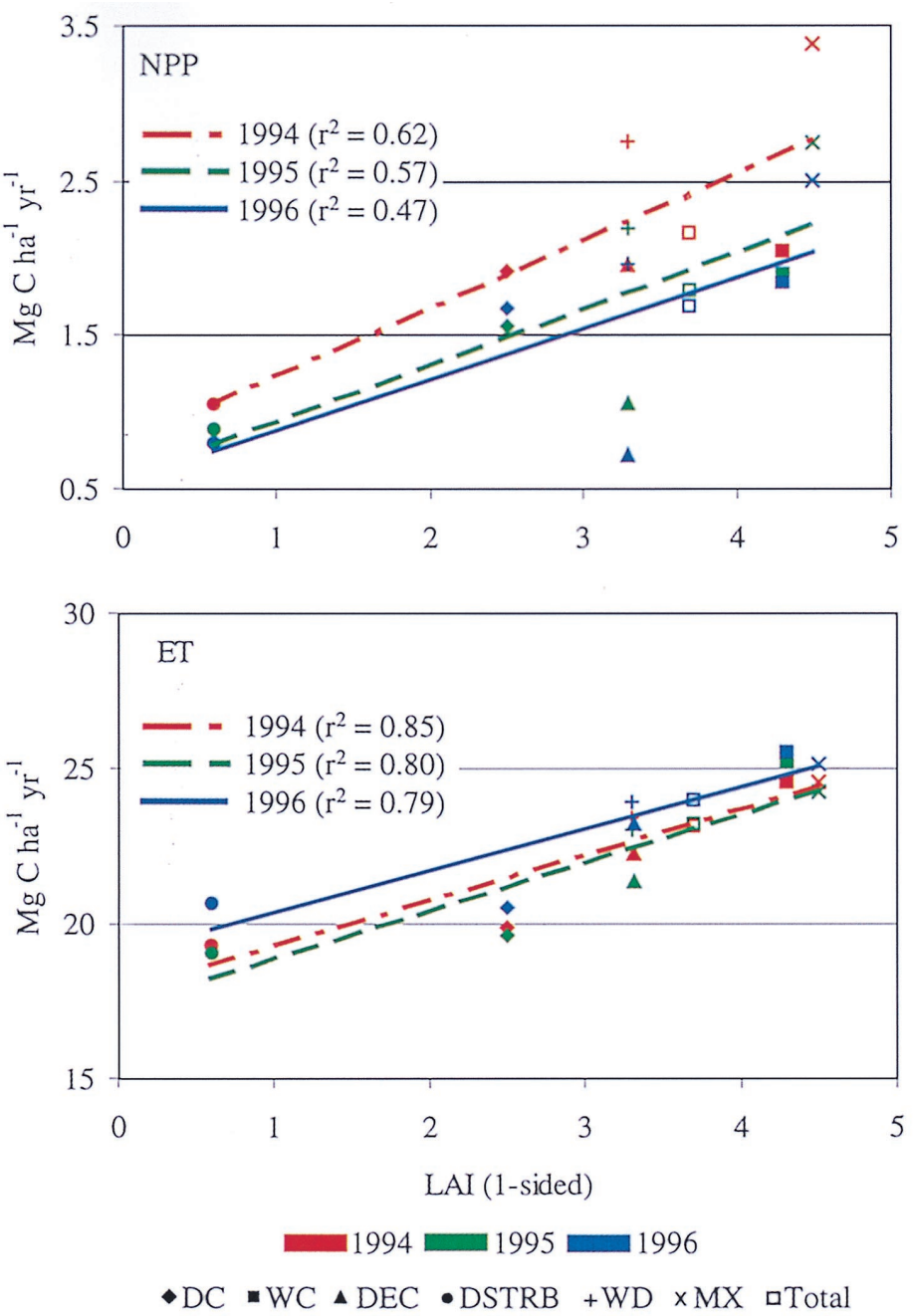

Plate 3. Plotted linear least squares relationships between LAI and BIOME-BGC (1994–1996) NPP (Mg C ha^{-1} yr^{-1}) and ET (cm yr^{-1}) simulations at the 30 m scale. Data points represent aerial means for the entire study region and individual land cover classes within the SMSA. LAI heterogeneity was a dominant factor influencing annual NPP and ET spatial complexity (see Plate 2, Table 3), while other biophysical differences between deciduous and coniferous vegetation were of secondary importance. Reductions in the height and slope of the NPP-LAI relationship for 1995 and 1996 were primarily due to marked reductions in annual productivity associated with cooler spring temperatures and simulated 3–4 week delays in leaf-out of deciduous vegetation. Annual ET showed greater association with LAI than annual NPP because ET characteristics between broadleaf deciduous and coniferous vegetation were found to behave similarly at longer timescales even though daily differences were often quite large.

found to have a major influence on scaling behavior. Careful consideration of landscape spatial and temporal heterogeneity is necessary to identify and mitigate potential error sources when using plot scale information to understand regional scale patterns.

Simulation of the seasonal cycles of atmospheric CO_2 at continental and global scales often involves the use of highly aggregated land cover data at spatial scales of 100 km^2 or more. Our results indicate that inadequate representation of sub-grid-scale land cover heterogeneity could significantly affect the timing and amplitude of the predicted seasonal CO_2 cycle. Underrepresentation of the proportions of broadleaf deciduous life-forms, for example, could result in overestimation of CO_2 uptake by the land surface in early spring, followed

by underestimation of maximum seasonal CO_2 uptake during the summer. Methods for mitigating these effects could involve the utilization of coarse scale data sets that incorporate information on dominant and subdominant land cover categories. Simulations could then be conducted by weighting each grid cell according to the relative proportions of the various land cover types represented.

There are other factors not addressed in this investigation which may also affect scaling behavior in water and carbon fluxes. First, our methods do not explicitly account for interactions between overstory and understory processes or lateral transfers of matter and energy. For example, lateral redistribution of runoff and soil moisture, as well as moss-overstory interactions may play an important role in mitigating or enhancing bias at regional scales. Other factors such as stand age, disease and mortality, and soil-nutrient variability were also not addressed in this investigation and may influence scaling behavior. Although much of the boreal forest is relatively flat, sub-grid-scale variability in precipitation, wind, solar irradiance, albedo, and the surface energy balance may induce greater heterogeneity in surface fluxes than we were able to distinguish using a 1 km resolution, gridded daily meteorological database, and a 30 m land cover database. Surface weather station information is currently limited in the BOREAS region and almost totally absent within global boreal forest and arctic regions. However, remote sensing information of surface characteristics such as biomass, freeze-thaw, albedo, and surface temperature may provide indirect "snapshots" of spatial heterogeneity in microclimate conditions and scaling behavior.

In recent years, developments in remote sensing technology, using arrays of different sensor platforms and instrument types, have produced an abundance of information about surface characteristics at a variety of spatial scales. Surface characteristics currently defined by remote sensing technology include both land cover (e.g., vegetation type, greenness, biomass, leaf area) and physical properties (e.g., surface temperature, freeze-thaw timing, and extent). All are potentially useful for describing spatial and temporal variations in surface conditions. Remote sensing information can be incorporated within an ecological process model framework to describe the function of boreal forest systems and disturbance-related effects on water and carbon cycling at a range of spatial scales. However, problems exist between linking patterns observed at one scale with processes and relationships identified at other scales. Careful consideration of landscape heterogeneity and scaling behavior is necessary to identify and mitigate potential error sources when using plot scale information to understand regional scale patterns. Remote sensing data integrated within an ecological process model framework provides an efficient mechanism to evaluate scaling behavior, interpret patterns in coarse resolution data, and identify appropriate scales of operation for various processes.

Acknowledgments. We express our thanks to NASA, BOREAS staff and science teams for providing ecological and remote sensing information for the BOREAS region. We also thank Peter Thornton, Joseph White, Alisa Keyser, Michael White, Saxon Holbrook, Kathy Hibbard, Galina Churkina, and Geoff Poole for helpful discussions. Optical remote sensing, land cover classification products were provided by the Canadian Center for Remote Sensing, CCRS through the BOREAS project. Meteorological data were provided by the Saskatchewan Research Council's AMS mesonet database and the National Climatic Data Center, NCDC. This study was funded under NASA grants NAG5-4923 and NAG-52297.

References

Acton, D. F., G. A. Padbury, and J. A. Shields, Soil landscapes of Canada-Saskatchewan digital map data: scale 1:1000000, CanSIS SK018200, version 90.11.30, CLBRR Arch. Agric. Can. Res. Branch, Ottawa, 1991.

Aerts, R., H. De Caluwe, and H. Konings, Seasonal allocation of biomass and nitrogen in four Carex species from mesotrophic and eutrophic fens affected by nitrogen supply, *J. Ecol.*, *80*, 653–664, 1992.

Baldocchi, D. D., C. A. Vogel, and B. Hall, Seasonal variation in carbon dioxide exchange rates above and below a boreal jack pine forest, *Agric. For. Meteorol.*, *83*, 147–170, 1997a.

Baldocchi, D. D., C. A. Vogel, and B. Hall, Seasonal variation of energy and water vapor exchange rates above and below a boreal jack pine forest canopy, *J. Geophys. Res.*, *102*, 28,939–28,951, 1997b.

Band, L. E., Effect of land surface representation on forest water and carbon budgets, *J. Hydrol.*, *150*, 749–772, 1993.

Betts, A. K., and J. H. Ball, Albedo over the boreal forest, *J. Geophys. Res.*, *102*, 28,901–28,909, 1997.

Bigger, C. M., and W. C. Oechel, Nutrient effect on maximum photosynthesis in arctic plants, *Holarc. Ecol.*, *5*, 158–163, 1982.

Black, T. A., G. den Hartog, H. H. Neumann, P. D. Blanken, P. C. Yang, C. Russell, Z. Nesic, X. Lee, S. G. Chen, and R. Staebler, Annual cycles of water vapour and carbon dioxide fluxes in and above a boreal aspen forest, *Global Change Biol.*, *2*, 219–229, 1996.

Bonan, G. B., Importance of leaf area index and forest type when estimating photosynthesis in boreal forests, *Remote Sens. Environ.*, *43*, 303–314, 1993.

Bonan, G. B., and H. H. Shugart, Environmental factors and ecological processes in boreal forests, *Annu. Rev. Ecol. Syst.*, *20*, 1–28, 1989.

BOREAS Science Team, *Boreal Atmosphere-Ecosystem Study*, *Experimental Plan*, version 3.1, NASA GSFC, Greenbelt, Md., 1995.

Chapin, F. S., G. R. Shaver, A. E. Giblin, K. J. Nadelhoffer, and J. A. Laundre, Responses of arctic tundra to experimental and observed changes in climate, *Ecology*, *76*(3), 694–711, 1995.

Chen, J. M., P. M. Rich, S. T. Gower, J. M. Norman, and S. Plummer, Leaf area index of boreal forests: Theory, techniques, and measurements, *J. Geophys. Res.*, *102*, 29,429–29,443, 1997.

Cosby, B. J., G. M. Hornberger, R. B. Clapp, and T. R. Ginn, A statistical exploration of the relationships of soil moisture characteristics to the physical properties of soils, *Water Resour. Res.*, *20*, 682–690, 1984.

Cuenca, R. H., D. E. Stangel, and S. F. Kelly, Soil water balance in a boreal forest, *J. Geophys. Res.*, *102*, 29,355–29,366, 1997.

Dang, Q.-L., H. A. Margolis, M. R. Coyea, M. Sy, and G. J. Collatz, Regulation of branch-level gas exchange of boreal trees: Roles of shoot water potential and vapor pressure difference, *Tree Physiol.*, *17*, 521–535, 1997a.

Dang, Q.-L., H. A. Margolis, M. Sy, M. R. Coyea, G. J. Collatz, and C. L. Walthall, Profiles of photosynthetically active radiation, nitrogen, and photosynthetic capacity in the boreal forest: Implications for scaling from leaf to canopy, *J. Geophys. Res.*, *102*, 28,845–28,859, 1997b.

Fan, S. M., M. L. Goulden, J. W. Munger, B. C. Daube, P. S. Bakwin, S. C. Wofsy, J. S. Amthor, D. R. Fitzjarrald, K. E. Moore and T. R. Moore, Environmental controls on the photosynthesis and respiration of a boreal lichen woodland: A growing season of whole-ecosystem exchange measurements by eddy correlation, *Oecologia*, *102*, 443–452, 1995.

Farquhar, G. D., and S. von Caemmerer, Modelling of photosynthetic response to environmental conditions, in *Encyclopedia of Plant Physiology*, *New Series*, vol. 12B, *Physiological Plant Ecology II*, edited by O. L. Lange, P. S. Nobel, C. B. Osmond, and H. Ziegler, pp. 549–587, Springer-Verlag, 1982.

Field, C., and H. A. Mooney, The photosynthesis-nitrogen relationship in wild plants, in *On the Economy of Plant Form and Function*, edited by T. J. Givnish, pp. 25–55, Cambridge Univ. Press, New York, 1986.

Goulden, M. L., et al., Sensitivity of boreal forest carbon balance to soil thaw, *Science*, *279*, 214–217, 1998.

Gower, S. T., J. Vogel, J. Norman, C. J. Kucharik, S. Steele, and T. K. Stow, Carbon distribution and above ground net primary production in aspen, jack pine, and black spruce stands in Saskatchewan and Manitoba, Canada, *J. Geophys. Res.*, *102*, 29,029–29,041, 1997.

Grier, C. C., K. A. Vogt, M. R. Keyes, and R. L. Edmonds, Biomass distribution and above- and belowground production in young and

mature *Abies amabilis* zone ecosystems of the Washington Cascades, *Can. J. For. Res*., *11*, 155–157, 1981.

Hall, F. G., D. E. Knapp, and K. F. Huemmrich, Physically based classification and satellite mapping of biophysical characteristics in the southern boreal forest, *J. Geophys. Res*., *102*, 29,567–29,580, 1997.

Hogg, E. H., and P. A. Hurdle, Sap flow in trembling aspen: Implications for stomatal responses to vapor pressure deficit, *Tree Physiol*., *17*, 501–509, 1997.

Hunt, R. E., and S. W. Running, Simulated dry matter yields for aspen and spruce stands in the North American boreal forest, *Can. J. Remote Sens*., *18*, 126–133, 1992.

Hunt, R. E., S. C. Piper, R. Nemani, C. D. Keeling, R. D. Otto, and S. W. Running, Global net carbon exchange and intra-annual atmospheric CO_2 concentrations predicted by an ecosystem process model and three-dimensional atmospheric transport model, *Global Biogeochem. Cycles*, *10*(3), 431–456, 1996.

Jarvis, P. G., J. M. Massheder, S. E. Hale, J. B. Moncrieff, M. Rayment, and S. L. Scott, Seasonal variation of carbon dioxide, water vapor, and energy exchanges of a boreal black spruce forest, *J. Geophys. Res*., *102*, 28,953–28,966, 1997.

Johnson-Flanagan, A. M., and J. N. Owens, Root respiration in white spruce (*Picea glauca* [Moench] Voss) seedlings in relation to morphology and environment, *Plant Physiol*., *81*, 21–25, 1986.

Kimball, J. S., P. E. Thornton, M. A. White, and S. W. Running, Simulating forest productivity and surface-atmosphere carbon exchange in the BOREAS study region, *Tree Physiol*., *17*, 589–599, 1997a.

Kimball, J. S., M. A. White, and S. W. Running, BIOME-BGC simulations of stand hydrologic processes for BOREAS, *J. Geophys. Res*., *102*, 29,043–29,051, 1997b.

Lavigne, M. B., and M. G. Ryan, Growth and maintenance respiration rates of aspen, black spruce and jack pine stems at northern and southern BOREAS sites, *Tree Physiol*., *17*, 543–551, 1997.

Matthews, E., Global vegetation and land use: New high-resolution databases for climate studies, *J. Clim. Appl. Meteorol*., *22*, 474–487, 1983.

Mitsch, W. J., and J. G. Gosselink, *Wetlands*, 2nd ed., Van Nostrand Reinhold, New York, 1983.

Myneni, R. B., C. D. Keeling, C. J. Tucker, G. Asrar, and R. R. Nemani, Increased plant growth in the northern high latitudes from 1981 to 1991, *Nature*, *386*, 698–702, 1997.

National Weather Service, Surface observations, *Fed. Meteorol. Handb. 1*, *FCM-H1-1988*, Off. of the Fed. Coord., Dep. of Comm., Washington, D. C., 1988.

Penning de Vries, F. W. T., A. Brunsting, and H. H. Van Laar, Products, requirements and efficiency of biosynthesis: A quantitative approach, *J. Theor. Biol*., *45*, 339–377, 1974.

Pierce, L. L., and S. W. Running, The effects of aggregating sub-grid land surface variation on large-scale estimates of net primary production, *Landscape Ecol*., *10*(4), 239–253, 1995.

Pierce, L. L., S. W. Running and J. Walker, Regional-scale relationships of leaf area index to specific leaf area and leaf nitrogen content, *Ecol. Appl*., *4*(2), 313–321, 1994.

Ranson, K. J., G. Sun, R. H. Lang, N. S. Chauhan, R. J. Cacciola, and O. Kilic, Mapping of boreal forest biomass from spaceborne synthetic aperature radar, *J. Geophys. Res*., *102*, 29,599–29,610, 1997.

Rastetter, E. B., A. W. King, B. J. Cosby, G. M. Hornberger, R. V. O'Neill, and J. E. Hobbie, Aggregating fine-scale ecological knowledge to model coarser-scale attributes of ecosystems, *Ecol. Appl*., *2*, 55–70, 1992.

Roulet, N. T., P. M. Crill, N. T. Comer, A. E. Dove, and R. A. Bourbonniere, CO_2 and CH_4 flux between a boreal beaver pond and the atmosphere, *J. Geophys. Res*., *102*, 29,313–29,319, 1997.

Running, S. W., and S. T. Gower, FOREST-BGC, a general model of forest ecosystem processes for regional applications, II, Dynamic carbon allocation and nitrogen budgets, *Tree Physiol*., *9*, 147–160, 1991.

Running, S. W., and R. E. Hunt, Generalization of a forest ecosystem process model for other biomes, BIOME-BGC, and an application for global-scale models, in *Scaling Physiologic Processes: Leaf to Globe*, edited by J. R. Ehleringer and C. B. Field, Academic, San Diego, Calif., 1993.

Running, S. W., R. R. Nemani, D. L. Peterson, L. E. Band, D. F. Potts, L. L. Pierce, and M. A. Spanner, Mapping regional forest evapotranspiration and photosynthesis by coupling satellite data with ecosystem simulation, *Ecology*, *70*(4), 1090–1101, 1989.

Saatchi, S., and M. Moghaddam, Estimation of crown and stem water content and biomass of boreal forest using polarimetric SAR imagery, *J. Geophys. Res*., in press, 1999a.

Saatchi, S., and M. Moghaddam, Developing a semi-empirical biomass estimation algorithm for polarimetric SAR data over boreal forest, *IEEE Trans. Geosci. Remote Sens*., in press, 1999b.

Saatchi, S. S., and E. Rignot, Classification of boreal forest cover types using SAR images, *Remote Sens. Environ*., *60*(3), 271–281, 1997.

Schimel, J. P., K. Kielland, and F. S. Chapin III, Nutrient availability and uptake by tundra plants, in *Landscape Function and Disturbance in Arctic Tundra*, edited by J. F. Reynolds and J. D. Tenhunen, pp. 203–213, Springer-Verlag, New York, 1996.

Sellers, P. J., Y. Mintz, Y. C. Sud, and A. Dalcher, A simple biosphere model (SiB) for use within general circulation models, *J. Atmos. Sci*., *43*(6), 305–331, 1986.

Sellers, P. J., M. D. Heiser, and F. G. Hall, Relationship between surface conductance and spectral vegetation indices at intermediate (100 m^2 to 15 km^2) length scales, *J. Geophys. Res*., *97*, 19,033–19,060, 1992.

Sellers, P. J., M. D. Heiser, F. G. Hall, S. J. Goetz, D. E. Strebel, S. B. Verma, R. L. Desjardins, P. M. Schuepp, and J. I. MacPherson, Effects of spatial variability in topography, vegetation cover and soil moisture on area-averaged surface fluxes: A case study using the FIFE 1989 data, *J. Geophys. Res*., *100*, 25,607–25,629, 1995.

Sellers, P. J., et al., BOREAS in 1997: Experiment overview, scientific results, and future directions, *J. Geophys. Res*., *102*, 28,731–28,769, 1997.

Shewchuk, S. R., Surface mesonet for BOREAS, *J. Geophys. Res*., *102*, 29,077–29,082, 1997.

Sprugel, D. G., M. G. Ryan, J. R. Brooks, K. A. Vogt, and T. A. Martin, Respiration from the organ level to the stand, in *Resource Physiology of Conifers, Acquisition, Allocation and Utilization*, edited by W. K. Smith and T. M. Hinckley, pp. 255–299, Academic, San Diego, Calif., 1995.

Steele, S. J., S. T. Gower, J. G. Vogel, and J. M. Norman, Root mass, net primary production and turnover in aspen, jack pine and black spruce forests in Saskatchewan and Manitoba, Canada, *Tree Physiol*., *17*, 577–587, 1997.

Steyaert, L. T., F. G. Hall, and T. R. Loveland, Land cover mapping, fire regeneration, and scaling studies in the Canadian boreal forest with 1 km AVHRR and Landsat TM data, *J. Geophys. Res*., *102*, 29,581–29,598, 1997.

Sullivan, J. H., B. D. Bovard, and E. M. Middleton, Variability in leaf-level CO_2 and water fluxes in Pinus banksiana and Picea mariana in Saskatchewan, *Tree Physiol*., *17*, 553–561, 1997.

Thornton, P. E., S. W. Running, and M. A. White, Generating surfaces of daily meteorological variables over large regions of complex terrain, *J. Hydrol*., *190*, 214–251, 1997.

Turner, D. P., R. Dodson, and D. Marks, Comparison of alternative spatial resolutions in the application of a spatially distributed biogeochemical model over complex terrain, *Ecol. Model*., *90*(1), 53–67, 1996.

Vogt, K., Carbon budgets of temperate forest ecosystems, *Tree Physiol*., *9*, 69–86, 1991.

Vowinckel, T., W. C. Oechel, and W. G. Boll, The effect of climate on the photosynthesis of Picea mariana at the subarctic tree line, 1, Field measurements, *Can. J. Bot*., *53*, 604–620, 1975.

Waring, R. H., and S. W. Running, *Forest Ecosystems Analysis at Multiple Scales*, Academic, San Diego, Calif., 1998.

White, M. A., P. E. Thornton, and S. W. Running, A continental phenology model for monitoring vegetation responses to interannual climatic variability, *Global Biogeochem. Cycles*, *11*, 217–234, 1997.

J. S. Kimball, Flathead Lake Biological Station, 311 BioStation Lane, Polson, MT 59860. (johnk@ntsg.umt.edu)

S. W. Running, Numerical Terradynamic Simulation Group, School of Forestry, University of Montana, Missoula MT 59001.

S. S. Saatchi, NASA Jet Propulsion Laboratory, Pasadena CA 91109.

(Received August 27, 1998; revised December 10, 1998; accepted February 4, 1999.)